Monthly Notices
of the
ROYAL ASTRONOMICAL SOCIETY

Mon. Not. R. Astron. Soc. **411,** 693–704 (2011) doi:10.1111/j.1365-2966.2010.17709.x

Mesoscale optical turbulence simulations above Dome C, Dome A and South Pole

F. Lascaux,[1⋆] E. Masciadri[1⋆] and S. Hagelin[1,2]

[1]*INAF Osservatorio Astrofisico di Arcetri, Largo Enrico Fermi 5, I-501 25 Florence, Italy*
[2]*Uppsala Universitet, Department of Earth Sciences, Villavägen 16, S-752 36 Uppsala, Sweden*

Accepted 2010 September 14. Received 2010 September 6; in original form 2010 June 16

ABSTRACT

In two recent papers, the mesoscale model Meso-NH, jointly with the Astro-Meso-NH package, has been validated at Dome C, Antarctica, for the characterization of optical turbulence. It has been shown that the meteorological parameters (temperature and wind speed, on which the optical turbulence depends) as well as the C_N^2 profiles above Dome C were correctly reproduced statistically. The three most important derived parameters that characterize the optical turbulence above the Internal Antarctic Plateau – the surface-layer thickness, the seeing in the free atmosphere and the seeing in the total atmosphere – were shown to be in very good agreement with observations. Validation of C_N^2 has been performed using all the measurements of the optical turbulence vertical distribution obtained in winter so far. In this paper, in order to investigate the ability of the model to discriminate between different turbulence conditions for site testing, we extend the study to two other potential astronomical sites in Antarctica: Dome A and South Pole, which we expect to be characterized by different turbulence conditions. The optical turbulence has been calculated above these two sites for the same 15 nights studied for Dome C and a comparison between the three sites has been performed. The ability of the Meso-NH model to discriminate between different types of optical turbulence behaviour is confirmed, and it is evident that the three sites considered have different characteristics as regards the seeing and the surface-layer thickness.

Key words: turbulence – atmospheric effects – site testing.

1 INTRODUCTION

The Internal Antarctic Plateau represents a potentially interesting location for astronomical applications. For almost a decade, astronomers have shown more and more interest towards this region of the Earth, thanks to its peculiar atmospheric conditions. The extreme cold temperature, the dry atmosphere and the facts that the plateau is at more than 2500 m above the sea level, the turbulence seems to develop mainly in a thin surface layer of the order of 30–40 m at the top of summits and the seeing above this surface layer assumes values comparable to those obtained at mid-latitude sites makes this region of the Earth very appealing for astronomers. South Pole was the first site equipped with an observatory in the Internal Antarctic Plateau in which measurements of the optical turbulence were carried out (Marks et al. 1996, 1999). 15 balloons were launched in the winter period and it was observed that the seeing above a surface layer of ∼220 m was very good (0.37 arcsec). Measurements of the optical turbulence at Dome C are more recent. After the first observations made in 2004 with a Multi-Aperture Scintillation Sensor (MASS) (Lawrence et al. 2004), a series of studies carried out with different instrumentation have been published that aim to provide an assessment of the integrated seeing (Aristidi et al. 2005, 2009) and the vertical distribution of the optical turbulence (Trinquet et al. 2008).

This paper deals with a different approach to site assessment. In this context we are interested in investigating the abilities of a mesoscale model (Meso-NH) in reconstructing the correct optical turbulence features above different sites of the Internal Antarctic Plateau and in discriminating between the optical turbulence properties of different sites. Meso-NH (Lafore et al. 1998) is a non-hydrostatic mesoscale research model developed jointly by the Centre National des Recherches Météorologiques (CNRM) and the Laboratoire d'Aérologie de Toulouse, France. The Astro-Meso-NH package (Masciadri, Vernin & Bougeault 1999a) was first proven to be able to reconstruct realistic C_N^2 profiles above astronomical sites (Masciadri, Vernin & Bougeault 1999b, 2001) and later statistically validated (Masciadri & Jabouille 2001; Masciadri, Avila & Sanchez 2004; Masciadri & Egner 2006). In the Astro-Meso-NH package, all the main integrated astroclimatic parameters such as the isoplanatic angle, wavefront coherence time, scintillation rate and spatial coherence outer scale are coded in the model (Masciadri

⋆E-mail: lascaux@arcetri.astro.it (FL); masciadri@arcetri.astro.it (EM)

Table 1. Results obtained in Lascaux et al. (2010a) that prove the Meso-NH model reliability above Dome C in reconstructing the optical turbulence spatial distribution. Three parameters are estimated: the mean surface turbulent layer (h_{sl}), the seeing in the free atmosphere (ε_{FA}) obtained by integrating C_N^2 from h_{sl} up to the end of the atmosphere, and the total seeing (ε_{TOT}) obtained by integrating C_N^2 from the ground up to the top of the atmosphere. Beside each parameter is reported the associated standard deviation (σ) and the statistical error ($\sigma/\sqrt{N}$).

	h_{sl} (m)	σ	$\sigma/\sqrt{N}$	ε_{FA} (arcsec)	σ	$\sigma/\sqrt{N}$	ε_{TOT} (arcsec)	σ	$\sigma/\sqrt{N}$
Observations	35.3	19.9	5.1	0.30	0.70	0.20	1.60	0.70	0.20
Model	44.2	24.6	6.6	0.30	0.67	0.17	1.70	0.77	0.21

et al. 1999a). The model is also coded to calculate the astroclimatic parameters in finite vertical slabs (h_{min}, h_{max}) in the troposphere (Masciadri et al. 1999a; Masciadri & Garfias 2001; Lascaux et al. 2010b). It can therefore be a useful tool for adaptive optics applications in classical as well as ground-layer adaptive optics (GLAO) and/or multi-conjugate adaptive optics (MCAO) configurations, because we can produce an optical turbulence vertical distribution in whatever vertical slab we wish and with suitable vertical resolution. More recently, Meso-NH was statistically validated above Dome C by Lascaux et al. (2009) and Lascaux, Masciadri & Hagelin (2010a). The most important results obtained in these two last papers are summarized in Table 1. Briefly, the observations at Dome C for a set of 15 winter nights (all available nights for which the optical turbulence vertical distribution is known) gave a mean surface-layer thickness $h_{sl,obs} = 35.3 \pm 5.1$ m. The simulated surface-layer thickness obtained with the Meso-NH model ($h_{sl,mnh} = 44.2 \pm 6.6$ m) is well correlated with measurements. The statistical error is of the order of 5–6 m but the standard deviation (σ) is of the order of 20–25 m. This indicates that the statistical fluctuation of this parameter is intrinsically quite important. The median simulated free-atmosphere seeing ($\varepsilon_{mnh,FA} = 0.30 \pm 0.17$ arcsec) as well as the median total seeing ($\varepsilon_{mnh,TOT} = 1.70 \pm 0.21$ arcsec) are well correlated with observations, respectively $\varepsilon_{obs,FA} = 0.3 \pm 0.2$ arcsec and $\varepsilon_{obs,TOT} = 1.6 \pm 0.2$ arcsec.

In the context of this paper, we consider that the Meso-NH model is calibrated as shown in Lascaux et al. (2010a), i.e. it produces optical turbulence features in agreement with observations. We therefore apply the Meso-NH model with the same configuration to two other sites on the plateau: South Pole and Dome A (Table 2).

Why these sites? Dome A is an almost uncontaminated site. It is the highest summit of the plateau and, for this reason, it is expected to be among the best astronomical sites for astronomical applications. The high altitude reduces the whole atmospheric path for light coming from space and above the summit the katabatic wind speed is reduced to minimum values. Dome A has been proven to have the strongest thermal stability (Hagelin et al. 2008) in proximity to the ground due to having the coldest temperature. Dome A is a Chinese base. In the last few years Chinese astronomers have given a new impulse to the site characterization, showing great interest in building astronomical facilities on this site. Optical turbulence measurements during the winter are not yet available but site-testing programmes are ongoing (Ashley et al. 2010). South Pole is interesting in our study because measurements of optical turbulence are available and, at the same time, the site is not located on a summit but on a gentle slope. From the preliminary measurements done in the past we expect a surface turbulent layer that is thicker than the surface layer that develops above the other two sites (Dome C and Dome A) due to the ground slope and the consequent katabatic winds in proximity to the surface. The three sites therefore form a perfect sample for a benchmark test of model behaviour and abilities.

In Section 2, the numerical set-up of the model is presented. In Section 3, results of the complete analysis of the three major parameters that characterize the optical turbulence features are reported: surface-layer thickness, seeing in the free atmosphere i.e. calculated above the surface layer and total seeing. Two different criteria to define the surface layer are used, with consequent double treatment. Finally, in Section 4 the results of this study are summarized.

2 NUMERICAL SET-UP

Meso-NH (Lafore et al. 1998) can simulate the temporal evolution of the three-dimensional atmospheric flow over any part of the globe. The prognostic variables forecast by this model are the three Cartesian components of the wind u, v, w, the dry potential temperature Θ, the pressure P and the turbulent kinetic energy *TKE*.

The system of equations is based upon an anelastic formulation, allowing for an effective filtering of acoustic waves. A Gal-Chen & Sommerville (1975) coordinate in the vertical and a C-grid in the formulation of Arakawa & Messinger (1976) for the spatial digitalization are used. The temporal scheme is an explicit three-time-level leap-frog scheme with a time filter (Asselin 1972). The turbulent scheme is a one-dimensional 1.5-closure scheme (Cuxart, Bougeault & Redelsperger 2000) with the Bougeault & Lacarrère (1989) mixing length. The surface exchanges are computed in an externalized surface scheme (SURFEX) including different physical packages, among them Interaction Soil Biosphere Atmosphere (ISBA; Noilhan & Planton 1989) for vegetation. Masciadri et al. (1999a,b) implemented the optical turbulence package in order to be able also to forecast the optical turbulence (C_N^2 3D maps) and

Table 2. Geographic coordinates of Dome A, Dome C and South Pole. The altitude is in m.

Site	Latitude	Longitude	Meso-NH altitude (m)	Measured altitude (m)
Dome A*	80°22′00″S	077°21′11″E	4089	4093
Dome C**	75°06′04″S	123°20′48″E	3230	3233
South Pole	90°00′00″S	000°00′00″E	2746	2835

*GPS measurement by Dr. X. Cui (private communication).
**GPS measurement by Prof. J. Storey (private communication).

Table 3. Meso-NH model configuration. The second column gives horizontal resolution ΔX, the third column the number of grid points and the fourth column the horizontal surface covered by the model domain.

Domain	ΔX (km)	Grid points	Surface (km × km)
Domain 1	25	120 × 120	3000 × 3000
Domain 2	5	80 × 80	400 × 400
Domain 3	1	80 × 80	80 × 80

all the astroclimatic parameters deduced from C_N^2. We will refer to the 'Astro-Meso-NH code' to indicate this package. The integrated astroclimatic parameters are calculated by integrating C_N^2 with respect to the zenith in the Astro-Meso-NH code. We list here the main characteristics of the numerical configuration used in this study.

(i) An interactive grid-nesting technique (Stein et al. 2000) is used, with three imbricated domains of increased horizontal mesh sizes ($\Delta X = 25$, 5 and 1 km, Table 3). Such a method is used to permit us to achieve the best resolution on a small surface but keep the volumetric domain in which the simulation is performed in thermodynamic equilibrium with the atmospheric circulation that evolves at large spatial scales in larger domains. We have shown (Lascaux et al. 2009) that the simulations result are sensitive to the chosen horizontal resolution. To achieve a good correlation between model output and observations, a grid-nesting configuration with a high horizontal resolution (at least $\Delta X = 1$ km) is mandatory.

(ii) The vertical grid is the same for all the domains reported in Table 3. The first vertical grid point is at 2 m above ground level (a.g.l.). A logarithmic stretched grid up to 3500 m a.g.l. (with 12 points in the first 100 m) is employed. Above 3500 m a.g.l., the vertical resolution is constant ($\Delta H \sim 600$ m). The maximum altitude achieved is around 20 km a.g.l. The first point at only 2 m above the ground (and with 12 points in the first 100 m) is necessary to forecast the typical very thin surface layer observed in the Antarctic Plateau.

(iii) All simulations are initialized and forced every 6 h at synoptic times (0000, 0600, 1200, 1800 UTC) by analyses from the European Centre for Medium-Range Weather Forecasts (ECMWF).[1] The simulations run for 18 h. Note that the time at which the simulation starts (UTC) differs for Dome A, Dome C and South Pole. This is done so as to be able to compare optical turbulence profiles simulated in the same temporal interval with respect to the local time (LT). For each night, a mean vertical profile of C_N^2 is computed between the time interval (2000–0000) LT as done in Lascaux et al. (2009, 2010a). This range is centred on the time at which the balloons were typically launched at Dome C. In this way we obtain the most representative simulated C_N^2 profile for each night. [2] In Table 4 are reported, for each site, the time at which the simulation starts and the duration ΔT of the simulation with respect to the local time.

(iv) An optimized version of the externalized surface-scheme ISBA for Antarctic conditions is employed (Le Moigne et al. 2009, 2010). Such a scheme has been used in Lascaux et al. (2010a) and contributed to providing a realistic reconstruction of the optical turbulence near the surface (optical turbulence strength and turbulence layer thickness). It is indeed obvious that the most critical part of an atmospheric model for this kind of simulation is the scheme that controls the air/ground turbulent fluxes budget. Our ability in reconstructing the surface temperature T_s well is related to our ability in reconstructing the sensible heat flux H, which is responsible of the buoyancy-driven turbulence in the surface layer.

(v) The Astro-Meso-NH package (Masciadri et al. 1999a) implemented in the most recent version of Meso-NH has been used to calculate the optical turbulence and derived astroclimatic parameters.

As shown in Lascaux et al. (2010a), the best choice for description of the orography is the Radarsat Antarctic Mapping Project (RAMP) Digital Elevation Model (DEM) presented in Liu et al. (2001), instead of the GTOPO30 DEM from the US Geological Survey used in Lascaux et al. (2009). For this study, therefore, the RAMP DEM has been used. The orography of each area of interest in this study (Dome C, Dome A, South Pole) is displayed in Fig. 1. All the grid-nested domains, from low horizontal resolution (larger mesh size) to high horizontal resolution (smaller mesh size), are reported. As can be seen in Fig. 1(c), (f) and (i), the orography around Dome C and Dome A is more detailed than the orography in proximity to the South Pole. This is due to the fact that the procedure to obtain a DEM integrates data from many different sources (satellite radar altimetry, airborne surveys, GPS surveys, station-based radar sounding, . . .). However the resolution of some areas (typically those that can barely receive information from the satellites) remains poorer than that of others. The region included in the inner circular polar region (and therefore South Pole) fits this condition, and this is the reason why the orography is somehow less detailed than for the rest of the Internal Antarctic Plateau. Nevertheless, this is a region with no peaks or mountains and with just a regular and gentle slope. We can therefore reasonably expect that the poorer accuracy in the orography has little or only minor influence on the results of the numerical simulations carried out with a mesoscale model such as Meso-NH.

The same set of 15 winter nights used by Lascaux et al. (2009, 2010a) to validate the model above Dome C is investigated in this study for the three Antarctic sites Dome C, Dome A and South Pole.

3 OPTICAL TURBULENCE ABOVE DOME C, DOME A AND SOUTH POLE

In this section we investigate and compare the values obtained above the three sites (Dome C, Dome A and South Pole) of three parameters that characterize the optical turbulence features above the Antarctic plateau:

(i) surface-layer thickness;

(ii) free-atmosphere seeing from the surface-layer thickness (h_{sl}) up to the top of the atmosphere;

(iii) total seeing from the ground up to the top of the atmosphere. We note that this corresponds to ∼10 km because the balloons explode at this altitude due to the high pressure and the strong wind speed.

[1] ECMWF: http://www.ecmwf.int/.

[2] In the prediction of a parametrized parameter (such as the optical turbulence) there is not a 1–1 correlation with the real time. This means, giving an explicit example, that is somehow meaningless to predict the turbulence at a precise time t=t* as we do for a parameter that we resolve explicitly such as the temperature or the wind speed. This is the reason why, in order to obtain the most representative C_N^2 profile to be compared with measurements, we calculate the mean of C_N^2 in a temporal interval ΔT. Such a procedure has been used in many previous papers (Masciadri & Jabouille 2001; Masciadri et al. 2004; Masciadri & Egner 2006).

Table 4. Simulation starting time and time interval chosen for C_N^2 computations for the three different sets of simulations (Dome A, Dome C and South Pole).

	Dome A	Dome C	South Pole
Starting time	0600 UTC/1100 LT	0000 UTC/0800 LT	1200 UTC/1200 LT
Time interval for C_N^2 computations (2000–0000 LT)	1500–1900 UTC	1200–1600 UTC	2000–0000 UTC

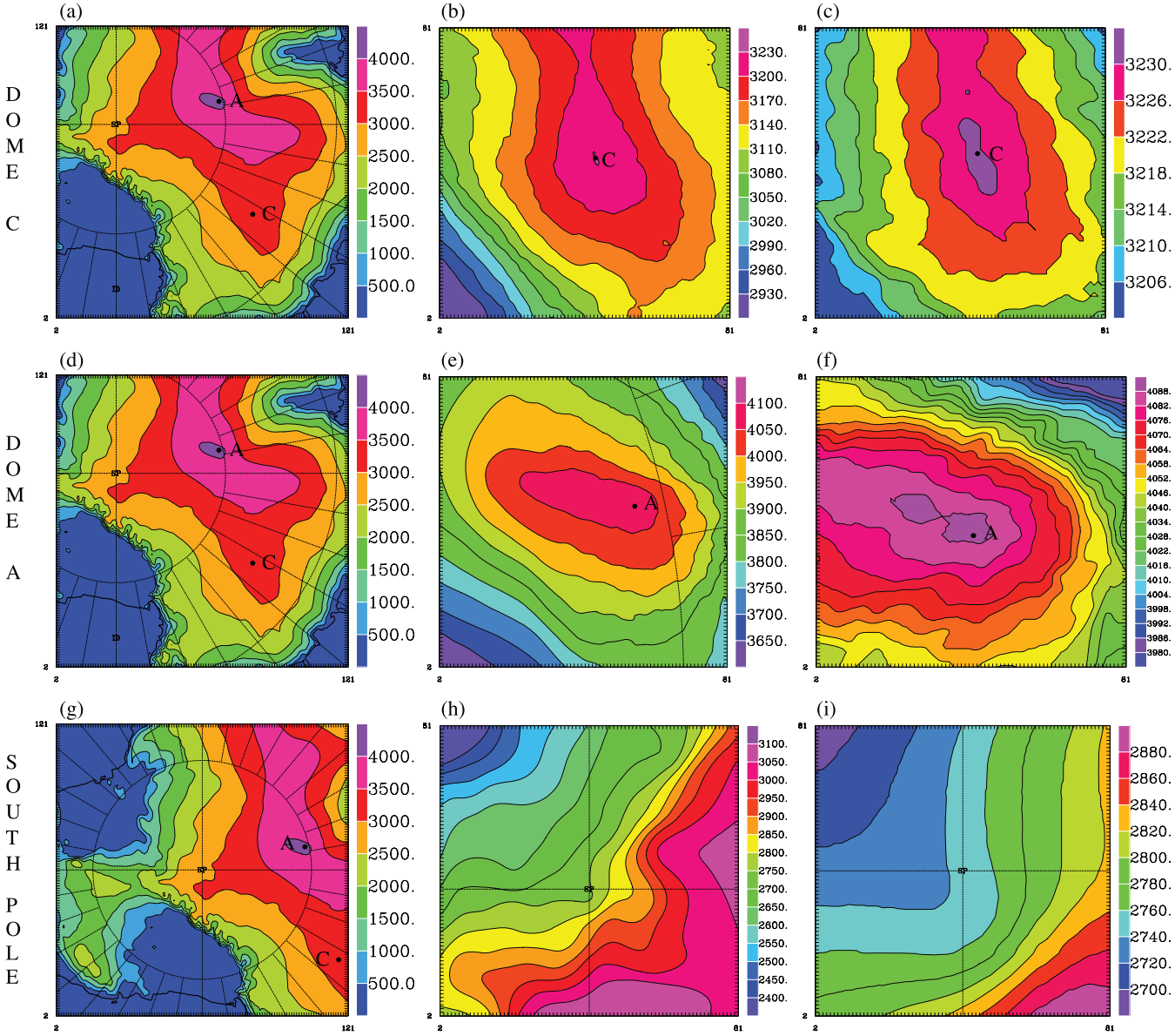

Figure 1. Orography of three different regions of the internal Antarctic Plateau as seen by the Meso-NH model (polar stereographic projection, grid-nesting configuration). (a), (b) and (c) show the three imbricated domains for the Dome C simulations, with horizontal resolution of 25, 5 and 1 km, respectively. (d), (e) and (f) show the three imbricated domains for the Dome A simulations, with horizontal resolution of 25, 5 and 1 km, respectively. (g), (h) and (i) show the three imbricated domains for the South Pole simulations, with horizontal resolution of 25, 5 and 1 km, respectively. The dot labelled 'C' indicates Concordia Station. The dot labelled 'A' indicates Dome A. SP stands for South Pole. The altitude is expressed in metres (m).

In a numerical mesoscale model, the great challenge and difficulty is related to the parametrization of the optical turbulence. The critical issue is related to the ability of the model in reconstructing the vertical distribution of the optical turbulence (i.e. C_N^2). This is the reason why we selected and studied these three fundamental parameters. The other integrated astroclimatic parameters are obtained by calculating the integral of C_N^2 and wind-speed vertical profiles along the troposphere. A forthcoming paper will be dedicated to the analysis of the integrated astroclimatic parameters.

Table 5. Mean surface-layer thicknesses h_{sl} computed for the three sites, for 15 different winter nights using the criterion in equation (1). Units in metres (m). The mean values are also reported, with the associated statistical error $\sigma/\sqrt{N}$.

Date	Dome A	Dome C	South Pole
2005 Jul 04	65.0	30.4	117.6
2005 Jul 07	529.4	35.4	262.9
2005 Jul 11	28.6	80.0	131.9
2005 Jul 18	27.7	49.7	224.0
2005 Jul 21	17.6	66.7	136.3
2005 Jul 25	15.7	27.4	298.6
2005 Aug 01	25.5	22.6	185.2
2005 Aug 08	53.1	34.2	104.4
2005 Aug 12	19.4	16.7	59.0
2005 Aug 29	17.4	91.4	251.3
2005 Sep 02	16.4	70.9	164.9
2005 Sep 05	125.2	338.4	128.0
2005 Sep 07	59.8	52.5	103.6
2005 Sep 16	38.8	19.4	158.7
2005 Sep 21	20.1	21.0	148.0
Mean	37.9*	44.2*	165.0
σ	30.2*	24.6*	67.3
$\sigma/\sqrt{N}$	8.1*	6.6*	17.4

*These values are computed without taking into account the night of 2005 September 5 for Dome C and the night of 2005 July 7 for Dome A (see text for further explanation).

3.1 Optical turbulence surface-layer thickness

To compute the surface-layer thickness for each night, the same method employed in Trinquet et al. (2008) and Lascaux et al. (2010a) is first used. The thickness h_{sl} is defined as the vertical slab containing 90 per cent of the optical turbulence developed inside the first km above the ground:

$$\frac{\int_{8m}^{h_{sl}} C_N^2(h)\,dh}{\int_{8m}^{1km} C_N^2(h)\,dh} < 0.90, \quad (1)$$

where C_N^2 is the refractive-index structure parameter. We recall here that the selection of this criterion (which we call criterion A) is motivated by the fact that we intend to compare our calculations with measurements made by Trinquet et al. (2008). This criterion has been selected by Trinquet et al. (2008) because the typical optical turbulence features above the Internal Antarctic Plateau are characterized by a major bump at the surface and a consistent decrease of the optical turbulence strength in the first tens of m. The selection of the percentage is obviously absolutely arbitrary and, in this context, is mainly useful to check the correlation with measurements and to compare predictions at different sites (in relative terms, therefore). The choice of the inferior limit of the integral (8 m) is motivated by the fact that Trinquet et al. (2008) intended to compare results obtained with balloons with those provided by the Differential Image Motion Monitor (DIMM) placed 8 m from the ground.

Table 5 reports the computed values of the surface-layer thickness for each night at the three sites, as well as the mean, standard deviation (σ) and statistical error ($\sigma/\sqrt{N}$) for the 15 nights. For each night, the surface-layer thickness is computed from a computed C_N^2 profile averaged between 2000 LT and 0000 LT (see Table 4 for times in UT), as done in Lascaux et al. (2010a). The calculated mean surface-layer thickness is $h_{sl} = 165 \pm 17.4$ m above South Pole, $h_{sl} = 44.2 \pm 6.6$ m at Dome C and $h_{sl} = 37.9 \pm 8.1$ m at Dome A. In this paper we are no longer forced to use the same inferior limit of the integral in equation (1) (8 m) as Trinquet et al. (2008), and we can compute the surface-layer thickness starting the integral at the ground. Under this assumption the calculated mean surface-layer thickness is $h_{sl} = 158.7 \pm 16.2$ m at South Pole, $h_{sl} = 45.0 \pm 7.1$ m at Dome C and $h_{sl} = 34.9 \pm 7.9$ m at Dome A. We conclude that at South Pole h_{sl} is more than three time larger than at Dome C or Dome A in both cases. This difference is well correlated with previous observations made above South Pole. More precisely, observations related to 15 balloons launched during the period 1995 June 20–August 18 indicated h_{sl} =220 m (Marks et al. 1999). Measurements in that paper are made in winter but in a different year and for different nights. It is not surprising therefore that the matching between calculations and measurements is not perfect. Unfortunately the precise dates of the nights studied in the paper of Marks et al. (1999) are not known. It is therefore not possible to provide a more careful estimate. It is, however, remarkable that the h_{sl} above South Pole is substantially larger than the h_{sl} above Dome C and Dome A. Also we note that the typical thickness calculated above South Pole with a statistical sample of three months by Swain & Gallée (2006) was $h_{sl} = 102$ m. The authors used a different definition of turbulent layer thickness, however. More precisely, they defined h_{sl} as the elevation (starting from the lowest model level) at which the turbulent kinetic energy contains 1 per cent of the turbulent kinetic energy of the lowest model layer. A comparison of this result with our calculations and with measurements is therefore meaningless. The same conclusion is valid for the estimates of h_{sl} given at Dome C as already explained in Lascaux et al. (2009, 2010a). In conclusion, looking at Table 5, individuals values for each night show a $h_{sl,SP}$ almost always higher than 100 m, with a maximum close to 300 m (2005 July 25), whereas $h_{sl,DC}$ and $h_{sl,DA}$ are always below 100 m. Dome C and Dome A have a comparable surface-layer thickness. For this sample of 15 nights, $h_{sl,DA}$ is 6.3 m smaller than $h_{sl,DC}$. We note also that the number of nights for which h_{sl} is very small (inferior at 30 m) is more important at Dome A (9 instead of 6 at Dome C). This difference is, however, not really statistically reliable considering the number of nights in the sample. For a more detailed discrimination between the h_{sl} value at Dome C and Dome A we need a larger statistic. This analysis is planned for a forthcoming paper.

Looking at the results obtained night by night, we can note some specific features observed in specific cases. Two nights (September 5 at Dome C ($h_{sl} = 338.4$ m) and July 7 at Dome A ($h_{sl} = 529.4$ m)) present similar characteristics: the surface-layer thickness h_{sl} is much larger than the observed one. In these two cases, however, as already explained in Lascaux et al. (2009, 2010a) for the case of Dome C, the large value of h_{sl} does not mean that a thicker and more developed turbulence is present near the ground but simply means that, in the first km from the ground, 90 per cent of the turbulence develops in the (0, h_{sl}) range. On September 5, at Dome C, the model reconstructs the total seeing over the whole 20 km as much weaker than has been observed and more uniformly distributed; consequently, the criterion (equation 1) provides us with a much larger value of h_{sl}. In both cases (on September 5 at Dome C and on July 7 at Dome A), when we look at the vertical distribution of C_N^2 calculated by the model, we observe that the turbulence is concentrated well below 20 m in a very thin surface layer with a very weak total seeing (see next section). The case of September 5 at Dome A is, however, a case in which the model reconstructed a surface turbulent layer thicker than has been observed.

It is known that a mesoscale model provide a temporal variability of the turbulence in the high part of the atmosphere that is smoother than observed with a vertical profiler. This is due to the fact that

Table 6. Mean surface-layer thicknesses h_{sl} computed for the three sites, for the same set of nights shown in Table 5 but computed with a different criterion. The surface-layer height is determined as the elevation at which the averaged TKE between 2000 LT and 0000 LT for each night is 1 per cent of the averaged lowest elevation value. Units in metres (m). The mean values are also reported, with the associated statistical error $\sigma/\sqrt{N}$.

Date	Dome A	Dome C	South Pole
2005 Jul 04	78*	32	112
2005 Jul 07	6*	32	112*
2005 Jul 11	40	76	174
2005 Jul 18	32	48	242
2005 Jul 21	22	56	144
2005 Jul 25	22	12*	148
2005 Aug 01	32	22	186
2005 Aug 08	56	32	112
2005 Aug 12	22	60	58
2005 Aug 29	22	82	250
2005 Sep 02	20	60	188
2005 Sep 05	136	30*	146
2005 Sep 07	72	74	250
2005 Sep 16	56	22	192
2005 Sep 21	26	22	170
Mean	42.8	44	165.6
σ	33.0	22.6	55.5
$\sigma/\sqrt{N}$	8.5	5.8	14.3

*These values are computed using a number of profiles smaller than five.

Table 7. Mean surface-layer thicknesses h_{sl} computed for the three sites, for the same set of nights shown in Table 5 but computed with a different criterion. The surface-layer height is determined as the elevation at which the averaged TKE between 2000 LT and 0000 LT for each night is 10 per cent of the averaged lowest elevation value. Units in metres (m). The mean values are also reported, with the associated statistical error $\sigma/\sqrt{N}$.

Date	Dome A	Dome C	South Pole
2005 Jul 04	58	22	56
2005 Jul 07	2	24	62
2005 Jul 11	28	52	64
2005 Jul 18	22	32	186
2005 Jul 21	14	40	110
2005 Jul 25	12	6	102
2005 Aug 01	22	16	126
2005 Aug 08	40	24	102
2005 Aug 12	16	8	40
2005 Aug 29	14	68	192
2005 Sep 02	14	46	112
2005 Sep 05	106	30	88
2005 Sep 07	50	52	68
2005 Sep 16	40	12	150
2005 Sep 21	18	14	116
Mean	30.4	27	104.9
σ	26.1	15.6	45.2
$\sigma/\sqrt{N}$	6.7	4	11.7

a mesoscale model is more active in the low part of the atmosphere, where orographic effects are mainly present. We recently obtained (Lascaux et al. 2009) very encouraging results showing that C_N^2 in the free atmosphere has a temporal variability even over a small dynamic range (-18, -16.5 on a logarithmic scale). This is a signature of the improvement of the model activity in the high part of the atmosphere. At present, however, it presents a hazard to quantifying the typical time-scale for temporal variability of all the parameters related to the optical turbulence reconstructed by a mesoscale model. Nevertheless we can describe the temporal variability of the morphology of these parameters, such as, for example, the thickness of the surface layer.

In Appendix A we report the temporal evolution of the calculated C_N^2 for all nights above the three sites. Looking at these results, we can give a description of the morphology of the temporal variation of the surface layer. Above Dome C and Dome A, the thickness of the surface layer remains mostly stable during the night, even though we have night-to-night variations as shown in Table 5. This fits with preliminary results shown in Ashley et al. (2010) above Dome A. Above South Pole, the thickness varies in a much more important way during the night, with oscillations that can reach 50–100 m. The larger variability of the typical turbulent surface-layer thickness is also confirmed by the larger value of σ observed above South Pole (Tables 5, 6 and 7).

In order to compare our calculations and results with those obtained by Swain & Gallée (2006), we also applied a different criterion (criterion B) based on the analysis of the vertical profile of turbulent kinetic energy (TKE) instead of the vertical profile of C_N^2. The TKE is certainly an ingredient on which the optical turbulence depends and it represents the dynamic turbulent energy. However, it is known (Masciadri & Jabouille 2001) that C_N^2 also depends on the gradient of the potential temperature, and moreover the selection of the value of the percentage of turbulent kinetic energy (1 per cent, 10 per cent, other) used as a threshold is absolutely arbitrary. This method is therefore not useful to quantify the absolute value of h_{sl} to be compared with measurements provided by Trinquet et al. (2008) and Marks et al. (1999). It could possibly be useful for relative comparisons between different sites or to compare our calculations with the calculations provided by Swain & Gallée (2006).

Using this method (Table 6), the surface-layer height is determined as the elevation at which the TKE is X per cent of the lowest elevation value. We calculated h_{sl} for $X = 1$ (Table 6) and $X = 10$ (Table 7). X=1 is the case treated by Swain & Gallée (2006). For each simulation, we first compute the average of the TKE profile for the night between 2000 LT and 0000 LT. While the average of the C_N^2 profile is calculated with a 2-min-rate sample, the average of the TKE is calculated with five profiles, available at each hour (2000, 2100, 2200, 2300, 0000 LT). This gives us an averaged vertical profile of the TKE characteristic of the considered night.

The computation of the surface-layer thickness is then performed using this averaged TKE profile. It has been observed that, when the night presents only low dynamic turbulence (with a very low averaged TKE at the lowest elevation level), it is very hard to retrieve a surface-layer height using this criterion. This means that the turbulence is so weak that we are at the limit of necessary turbulent kinetic energy to resolve the turbulence itself. For these nights (indicated with an asterisk in Table 6) it could happen that we calculated the average using a number of estimates smaller than 5 (as for all the other cases). The results are reported in Table 6.

Table 6 shows that results obtained with the TKE criterion are similar to those obtained with the criterion described in equation (1). Table 7 provides smaller values of h_{sl} above all three sites. We treat the case $X = 10$ to show that, by tuning the value of the percentage, it is possible to find different values of h_{sl}. This means that h_{sl} estimates are useful only if they are compared with measurements using the same criteria.

To conclude, both criteria (A and B with X=1) give similar mean h_{sl} values for all 3 sites for this limited set of nights. Evaluating the

Table 8. Total seeing $\varepsilon_{\rm TOT} = \varepsilon_{[8{\rm m},h_{\rm top}]}$ and seeing in the free atmosphere $\varepsilon_{\rm FA} = \varepsilon_{[h_{\rm sl},h_{\rm top}]}$ calculated for the 15 nights and averaged in the temporal range 2000–0000 LT. See the text for the definition of $h_{\rm sl}$ and $h_{\rm top}$.

Date	Dome A $\varepsilon_{\rm FA}/\varepsilon_{\rm TOT}$ ($h_{\rm sl} = 37.9$ m)	Dome C $\varepsilon_{\rm FA}/\varepsilon_{\rm TOT}$ ($h_{\rm sl} = 44.2$ m)	South Pole $\varepsilon_{\rm FA}/\varepsilon_{\rm TOT}$ ($h_{\rm sl} = 165$ m)
2005 Jul 04	2.55/3.37	0.22/2.28	0.40/1.67
2005 Jul 07	0.20/0.24	0.28/1.91	0.31/0.70
2005 Jul 11	0.23/2.78	1.61/1.81	0.47/1.96
2005 Jul 18	0.21/2.73	0.80/1.94	1.46/2.28
2005 Jul 21	0.21/1.95	0.86/1.27	0.31/1.71
2005 Jul 25	0.22/1.55	0.25/0.85	0.32/0.76
2005 Aug 01	0.22/1.78	0.22/2.27	0.52/1.78
2005 Aug 08	1.45/2.42	0.35/1.70	0.28/1.69
2005 Aug 12	0.23/2.37	0.23/0.99	0.29/1.82
2005 Aug 29	0.23/1.83	2.29/2.47	1.55/2.11
2005 Sep 02	0.22/1.76	1.16/1.54	0.81/3.56
2005 Sep 05	3.21/3.36	0.30/0.52	0.31/2.98
2005 Sep 07	2.43/3.49	1.69/3.73	0.31/1.41
2005 Sep 16	1.11/4.60	0.21/1.57	0.99/3.96
2005 Sep 21	0.20/2.30	0.26/1.63	0.36/2.32
Median	0.23/2.37	0.30/1.70	0.36/1.82
σ	1.08/1.03	0.67/0.77	0.43/0.90
$\sigma/\sqrt{N}$	0.28/0.27	0.17/0.21	0.11/0.23

surface-layer thickness over a more extended set of nights should be the next step. It would permit us to compute more reliable and robust statistical estimates for $h_{\rm sl}$ over the three Antarctic sites and possibly to discriminate between the $h_{\rm sl}$ at Dome A and Dome C. This also means that our estimate of $h_{\rm sl}$=165 m above South Pole is better correlated with measurements ($h_{\rm sl}$ =220 m) than the estimate ($h_{\rm sl}$ = 102 m) obtained by Swain & Gallée (2006) at the same site.

3.2 Seeing in the free atmosphere and the whole atmosphere

The seeing in the free atmosphere and in the whole atmosphere for $\lambda = 0.5 \times 10^{-6}$ m are

$$\varepsilon_{\rm FA} = 5.41\,\lambda^{-1/5}\left(\int_{h_{\rm sl}}^{h_{\rm top}} C_N^2(h)\,{\rm d}h\right)^{3/5} \quad (2)$$

and

$$\varepsilon_{\rm TOT} = 5.41\,\lambda^{-1/5}\left(\int_{8{\rm m}}^{h_{\rm top}} C_N^2(h)\,{\rm d}h\right)^{3/5}, \quad (3)$$

with $h_{\rm top} \sim 13$ km from sea level, i.e. where the balloons explode and we no longer have their signal. Table 8 shows the simulated total seeing ($\varepsilon_{\rm TOT}$) and free-atmosphere seeing ($\varepsilon_{\rm FA}$) for each night and each site (Dome C, Dome A and South Pole). We define the free atmosphere as the portion of the atmosphere extended from the mean $h_{\rm sl}$ reported in Table 5 up to $h_{\rm top}$. The median values of the seeing as well as the standard deviation (σ) and the statistical error ($\sigma/\sqrt{N}$) are reported. As expected, the total seeing is stronger at Dome A ($\varepsilon_{\rm TOT,DA} = 2.37 \pm 0.27$ arcsec) than at Dome C ($\varepsilon_{\rm TOT,DC} = 1.70 \pm 0.21$ arcsec) or South Pole ($\varepsilon_{\rm TOT,SP} = 1.82 \pm 0.23$). The total seeing is very well correlated with measurements at Dome C (Lascaux et al. 2010a: $\varepsilon_{\rm TOT,obs} = 1.6$ arcsec) and at South Pole (Marks et al. 1999: $\varepsilon_{\rm TOT,obs} = 1.86$ arcsec), making the estimate at Dome A highly reliable. The minimum median free-atmosphere seeing is found at Dome A ($\varepsilon_{\rm FA,DA} = 0.23 \pm 0.28$ arcsec). The median free-atmosphere seeing at Dome C is $\varepsilon_{\rm FA,DC} = 0.30 \pm 0.17$ arcsec and at South Pole $\varepsilon_{\rm FA,SP} = 0.36 \pm 0.11$ arcsec. The seeing in the free atmosphere is very well correlated with measurements at Dome C (Lascaux et al. 2010a: $\varepsilon_{\rm FA,obs} = 0.30$ arcsec) and at South Pole (Marks et al. 1999: $\varepsilon_{\rm FA,obs} = 0.37$ arsec), again making the method (Meso-NH model) as well as the estimates at Dome A very reliable. What is remarkable is that, even if $h_{\rm sl,DA} < h_{\rm sl,DC} < h_{\rm sl,SP}$, Dome A is the site with the lowest free-atmosphere seeing $\varepsilon_{\rm FA}$. This means that at Dome A, as well as at Dome C, the turbulence is concentrated inside the first tens of m from the ground. Moreover, the turbulence in the surface layer is stronger at Dome A than at Dome C. This can be explained with reference to the stronger thermal stability of Dome A near the ground. Our results therefore match the predictions made in Hagelin et al. (2008), who studied only features of the meteorological parameters.

At South Pole, however, the C_N^2 vertical distribution decreases in a less abrupt way because the thermal stability near the ground is less important. The C_N^2 vertical distribution is spread over hundreds of m from the ground, instead of tens of m as for Dome A or Dome C. As a consequence, the total seeing is also weaker than above Dome C and Dome A.

Such a behaviour is evidenced in Fig. 2, which displays the median vertical C_N^2 profiles over the three sites.

Looking at Table 8, we note that the values of σ for the total seeing above the three sites are mostly comparable with no significant differences, even if the Dome C value seems a little smaller (0.77) than those for Dome A (1.03) and South Pole (0.90). This indicates a comparable variability of the turbulence above the three sites. Concerning the seeing in the free atmosphere, the value of σ above Dome A is almost double (1.08) that above Dome C (0.67) and South Pole (0.43).

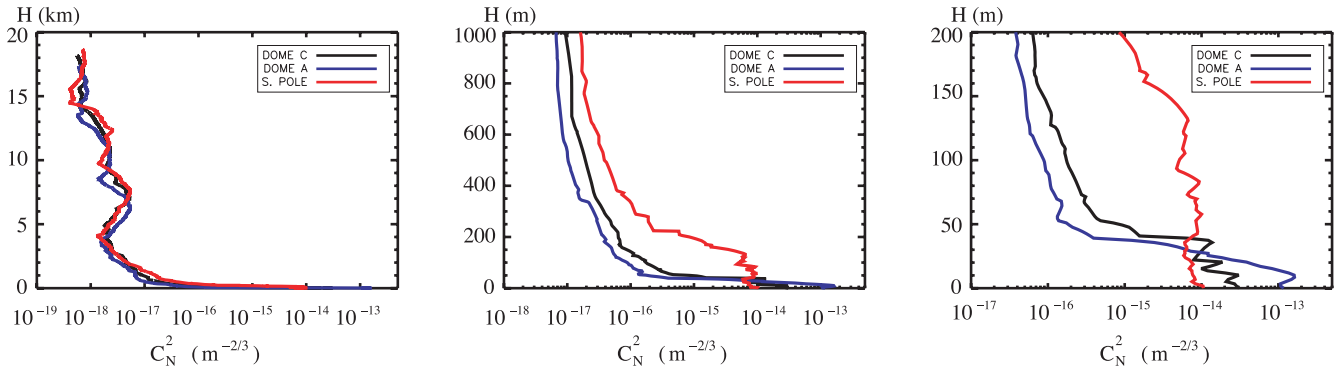

Figure 2. Median C_N^2 profiles simulated with the Meso-NH mesoscale model at Dome C, Dome A and South Pole. Left: from the ground up to 20 km. Middle: from the ground up to 1 km. Right: from the ground up to 200 m. Units are m$^{-2/3}$.

Table 9. Summary of the main results obtained in this study: surface layer h_{sl}, seeing in the free atmosphere (ε_{FA}) and total seeing (ε_{TOT}) at Dome C, Dome A and South Pole. The associated standard deviation (σ) and the statistical error ($\sigma/\sqrt{N}$) are also reported.

	h_{sl} (m)	σ	$\sigma/\sqrt{N}$	ε_{FA} (arcsec)	σ	$\sigma/\sqrt{N}$	ε_{TOT} (arcsec)	σ	$\sigma/\sqrt{N}$
Observations – Dome C	35.3	19.9	5.1	0.30	0.70	0.20	1.60	0.70	0.20
Meso-NH – Dome C	44.2	24.6	6.6	0.30	0.67	0.17	1.70	0.77	0.21
Meso-NH – Dome A	37.9	30.2	8.1	0.23	1.08	0.28	2.37	1.03	0.27
Meso-NH – South Pole	165.0	67.3	17.4	0.36	0.43	0.11	1.82	0.90	0.23

4 CONCLUSION

In this study, the mesoscale model Meso-NH was used to perform forecasts of optical turbulence (evolution of C_N^2 profiles) for 15 winter nights at three different Antarctic sites: Dome A, Dome C and South Pole. The model has been used with the same configuration previously validated at Dome C (Lascaux et al. 2010a) and simulations of the same 15 nights have been performed above the three sites. The idea behind our approach is that once validated above Dome C, the model can be used above two other sites of the Internal Antarctic Plateau to discriminate between optical turbulence features typical of these other sites. This should show the potential of the numerical tool in the context of site selection and characterization in astronomy. South Pole has been chosen because in the past some measurements of the optical turbulence have been done and this can represent a useful constraint on the model itself. For Dome A there are no measurements of the optical turbulence at present and this study therefore provides the first estimates ever made of the optical turbulence above this site. We test this approach above the Antarctic plateau, because this region is particularly simple from the topographic point of view and certainly simpler than typical mid-latitude astronomical sites. No major mountain chains are present and the local surface circulations are mainly addressed by the energy-budget air/ground transfer, the polar-vortex circulation at synoptic scales and the katabatic winds generated by gravity effects on gentle slopes due to the low temperature of the iced surface. The main results we obtained are summarized in Table 9 and listed here.

(i) We provide the first estimate of the optical turbulence extended over the whole 20 km above the Internal Antarctic Plateau.

(ii) The Meso-NH model achieves a reconstruction of the three most important parameters used to characterize the optical turbulence: the turbulent surface-layer thickness, the seeing in the free atmosphere and seeing in the surface layer for the three selected sites (Dome C, Dome A and South Pole), showing results in agreement with expectations. Measurements taken at Dome C and South Pole correspond to balloons launched during 15 nights, in both cases. This statistic is not very large, but reliable for a first significant result. The selected nights correspond to the 15 nights for which measurements of Dome C are available.

(iii) Dome C and Dome A present a very thin surface-layer size ($h_{sl,DA} = 37.9 \pm 8.1$ m and $h_{sl,DC} = 44.2 \pm 6.6$ m), while the South Pole surface layer is much thicker ($h_{sl,SP} = 165 \pm 17.4$ m). If we apply the criterion (A) described by equation (1), integrating from the ground instead of 8 m from the ground, we find a similar result within a couple of m. All these estimates are well correlated with measurements. Surface layers calculated by the model at Dome C and Dome A have a comparable thickness considering the actual sample. To discriminate better between the Dome A and Dome C surface-layer thicknesses, a richer statistic is necessary. An ongoing study has started addressing this issue.

(iv) Dome A is the site with the strongest total seeing (2.37 ± 0.27 arcsec) with respect to Dome C ($\varepsilon_{TOT,DC} = 1.70 \pm 0.21$ arcsec) and South Pole ($\varepsilon_{TOT,SP} = 1.82 \pm 0.23$ arcsec). This is explained by the stronger thermal stability near the ground with respect to the other two sites, which causes large values of the optical turbulence in the thin surface layer.

(v) All three sites show a very weak seeing in the free atmosphere, i.e. above the corresponding mean h_{sl}: $\varepsilon_{FA,DA} = 0.23 \pm 0.28$ arcsec at Dome A, $\varepsilon_{FA,DC} = 0.30 \pm 0.17$ arcsec at Dome C and $\varepsilon_{FA,SP} = 0.36 \pm 0.11$ arcsec at South Pole. Dome A shows the weakest seeing in the free atmosphere.

(vi) The temporal variability of the thickness of the surface layer is more important at South Pole than above Dome A and Dome C, which show very stable trends in agreement with observations. The temporal variability of the seeing in the whole atmosphere does not show important differences above the three sites, while the variability of the seeing in the free atmosphere at Dome A is almost double that at Dome C and South Pole.

(vii) Both the total seeing and the seeing in the free atmosphere calculated by Meso-NH are very well correlated with measurements at Dome C and South Pole, making the predictions made at Dome A highly reliable.

(viii) Dealing with the criteria used to define the surface-layer thickness, we proved that, at least for the sample of 15 nights investigated, the criterion defined by equation (1) (criterion A) and the criterion using the vertical profile of the turbulent kinetic energy (TKE) taking h_{sl} as the height at which the value of the TKE is less than 1 per cent of the TKE at the lowest level near the ground (criterion B) provide very similar results.

(ix) The mean h_{sl} estimated at Dome C (h_{sl}=44.2) is slightly thicker than that found by Swain & Gallée (2006) (h_{sl} =27.7 m), with a comparable discrepancy from measurements ($h_{sl} = 35.3 \pm 5.1$ m). The h_{sl} estimated at South Pole ($h_{sl,SP} = 165 \pm 17.4$ m) is thicker than that estimated by Swain & Gallée (2006) ($h_{sl,SP} = 102$) but better correlated with measurements ($h_{sl,SP} = 220$ m) than was found by Swain & Gallée (2006). The h_{sl} we estimate at Dome A ($h_{sl,DA} = 37.9 \pm 8.1$ m) is somehow thicker than that estimated by Swain & Gallée (2006) ($h_{sl,DA} = 18$ m). It is, however, important to note that the standard deviation of h_{sl} is of the order of h_{sl} itself or even larger. The statistical error $\sigma/\sqrt{(N)}$ is of the order of $\sim$10 m. We think therefore that at present there are no major differences between our results and those of Swain & Gallée (2006), with the exception of the fact that we proved that, with our model, the horizontal resolution of 1 km provides better results than the resolution of 100 km that is used by Swain & Gallée (2006).

All these results deserve confirmation provided by an analysis performed with a richer statistical sample. It would also be interesting to refine this study when optical turbulence measurements above Dome A are published. This aside, we can state that all major expectations concerning the typical features of the optical

turbulence above South Pole, Dome C and Dome A have been confirmed by this study. The tendency shown by the model is obviously that in summer time in proximity to the surface, due to the less stable regime, the turbulence thickness increases but the turbulence strength decreases. This is, however, outside the scope of this paper.

ACKNOWLEDGMENTS

ECMWF products are extracted from the catalogue MARS, http://www.ecmwf.int, and access to these data was authorized by the Meteorologic Service of the Italian Air Force. This study has been funded by the Marie Curie Excellence Grant (FOROT) – MEXT-CT-2005-023878.

REFERENCES

Arakawa A., Messinger F., 1976, GARP Techical Report 17. WMO/ICSU, Geneva, Switzerland
Aristidi E. et al., 2005, A&A, 444, 651
Aristidi E. et al., 2009, A&A, 499, 955
Ashley M. et al., 2010, EAS Publ. Ser., 40, 79
Asselin R., 1972, Mon. Weather Rev., 100, 487
Bougeault P., Lacarrère P., 1989, Mon. Weather Rev., 117, 1972
Cuxart J., Bougeault P., Redelsperger J.-L., 2000, Q. J. R. Meteorol. Soc., 126, 1
Gal-Chen T., Sommerville C. J., 1975, J. Comput. Phys., 17, 209
Hagelin S., Masciadri E., Lascaux F., Stoesz J., 2008, MNRAS, 387, 1499
Lafore J.-P. et al., 1998, Ann. Geophys., 16, 90
Lascaux F., Masciadri E., Stoesz J., Hagelin S., 2009, MNRAS, 398, 1093
Lascaux F., Masciadri E., Hagelin S., 2010a, MNRAS, 403, 1714
Lascaux F., Masciadri E., Hagelin S., 2010b, in Stepp L. M., Gilmozzi R., Hall H. J., eds, Proc. SPIE Vol. 7733, Ground-based and Airborne Telescopes III. SPIE, Bellingham, p. 77334E
Lawrence J., Ashley M., Tokovinin A., Travouillon T., 2004, Nat, 431, 278
Le Moigne P., Noilhan J., Masciadri E., Lascaux F., Pietroni I., 2009, in-Masciadri, E., Sarazin, M., eds, Optical Turbulence – Astronomy meets Meteorology. Imperial College Press, London, p. 165
Le Moigne P., Noilhan J., Masciadri E., Lascaux F., Pietroni I., 2010, J. Geophys. Res., submitted
Liu H., Jezek K., Li B., Zhao Z., 2001, Radarsat Antarctic Mapping Project Digital Elevation Model, V. 2. Digital media. National Snow and Ice Data Center, Boulder, CO, USA
Marks R. D., Vernin J., Azouit M., Briggs J. W., Burton M. G., Ashley M. C. B., Manigault J. F., 1996, A&A, 118, 385
Marks R. D., Vernin J., Azouit M., Manigault J. F., Clevelin C., 1999, A&AS, 134, 161
Masciadri E., Egner S., 2006, PASP, 118, 1604
Masciadri E., Garfias T., 2001, A&A, 366, 708
Masciadri E., Jabouille P., 2001, A&A, 376, 727
Masciadri E., Vernin J., Bougeault P., 1999a, A&ASS, 137, 185
Masciadri E., Vernin J., Bougeault P., 1999b, A&ASS, 137, 203
Masciadri E., Vernin J., Bougeault P., 2001, A&A, 365, 699
Masciadri E., Avila R., Sanchez L. J., 2004, Rev. Mex. Astron. Astrofis., 40, 3
Noilhan J., Planton S., 1989, Mon. Weather Rev., 117, 536
Stein J., Richard E., Lafore J.-P., Pinty J.-P., Asencio N., Cosma S., 2000, Meteorol. Atmos. Phys., 72, 203
Swain M., Gallée H., 2006, PASP, 118, 1190
Trinquet H., Agabi K., Vernin J., Azouit M., Aristidi E., Fossat E., 2008, PASP, 120, 203

APPENDIX A: COMPUTED TEMPORAL EVOLUTION OF C_N^2 VERTICAL PROFILES FOR EACH NIGHT AT DOME C, DOME A AND SOUTH POLE

In this Appendix we present all individual figures of the 18-h temporal evolution of C_N^2 for every night and at the three Antarctic sites considered in this study (Fig. A1: Dome A; Fig. A2: Dome C; Fig. A3: South Pole). The first couple of hours can be considered as spurious because of the model adaptation to the ground.

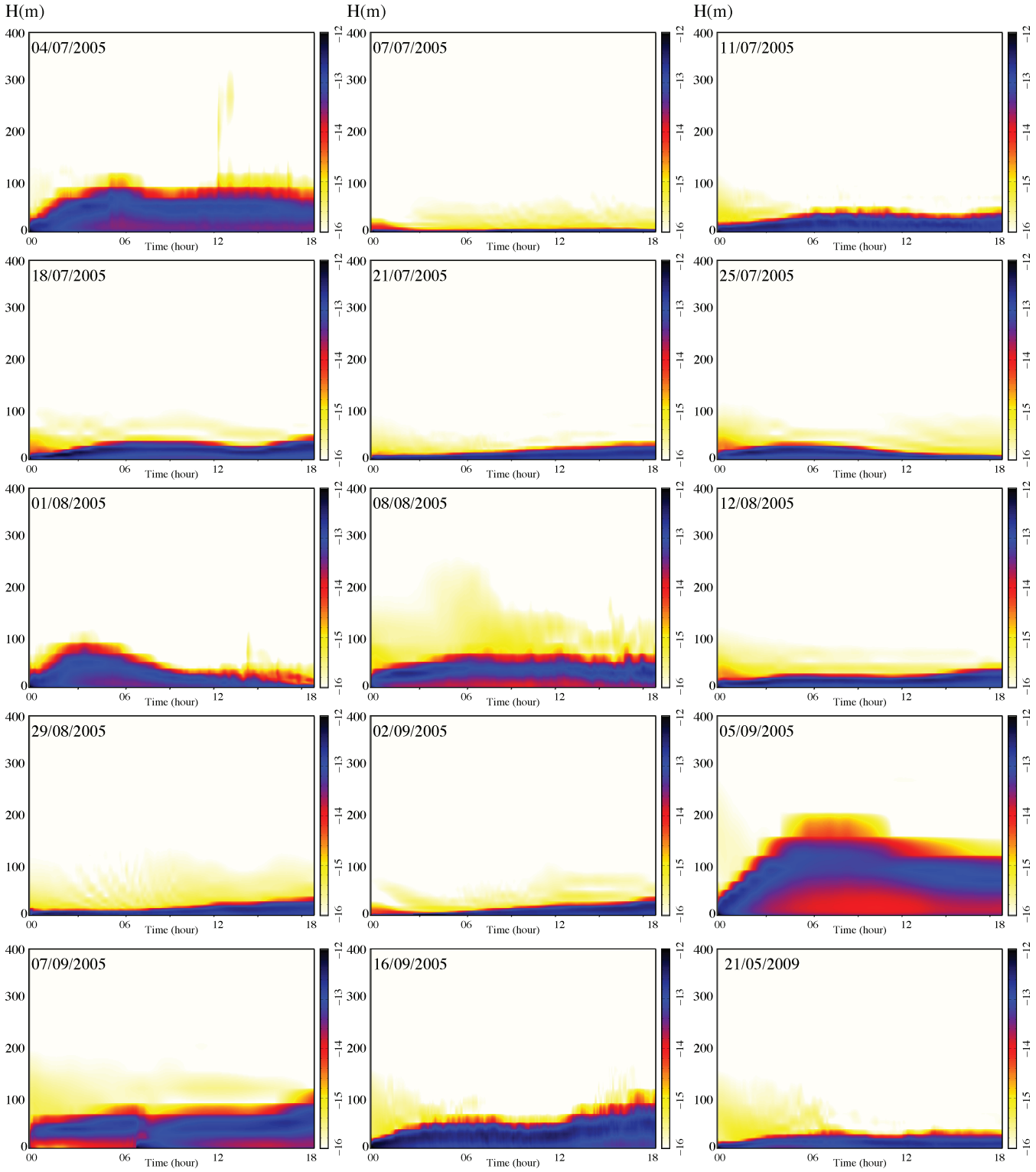

Figure A1. Meso-NH temporal evolution of C_N^2 vertical profiles at Dome A (log units) for the 15 forecast nights, for all 18 h of the simulations, from the ground up to 400 m above ground level. Units are $m^{-2/3}$.

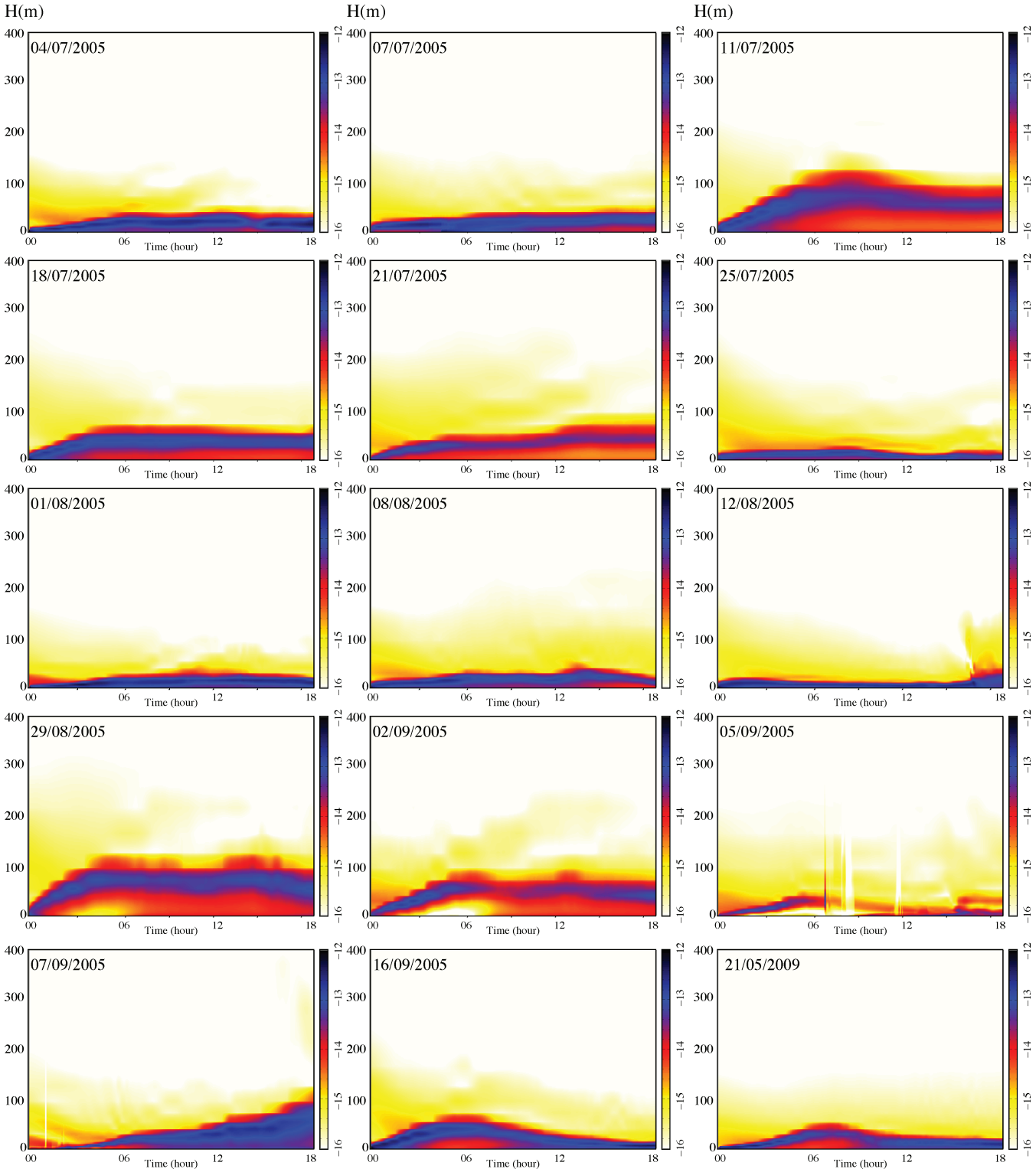

Figure A2. As Fig. A1 but for Dome C.

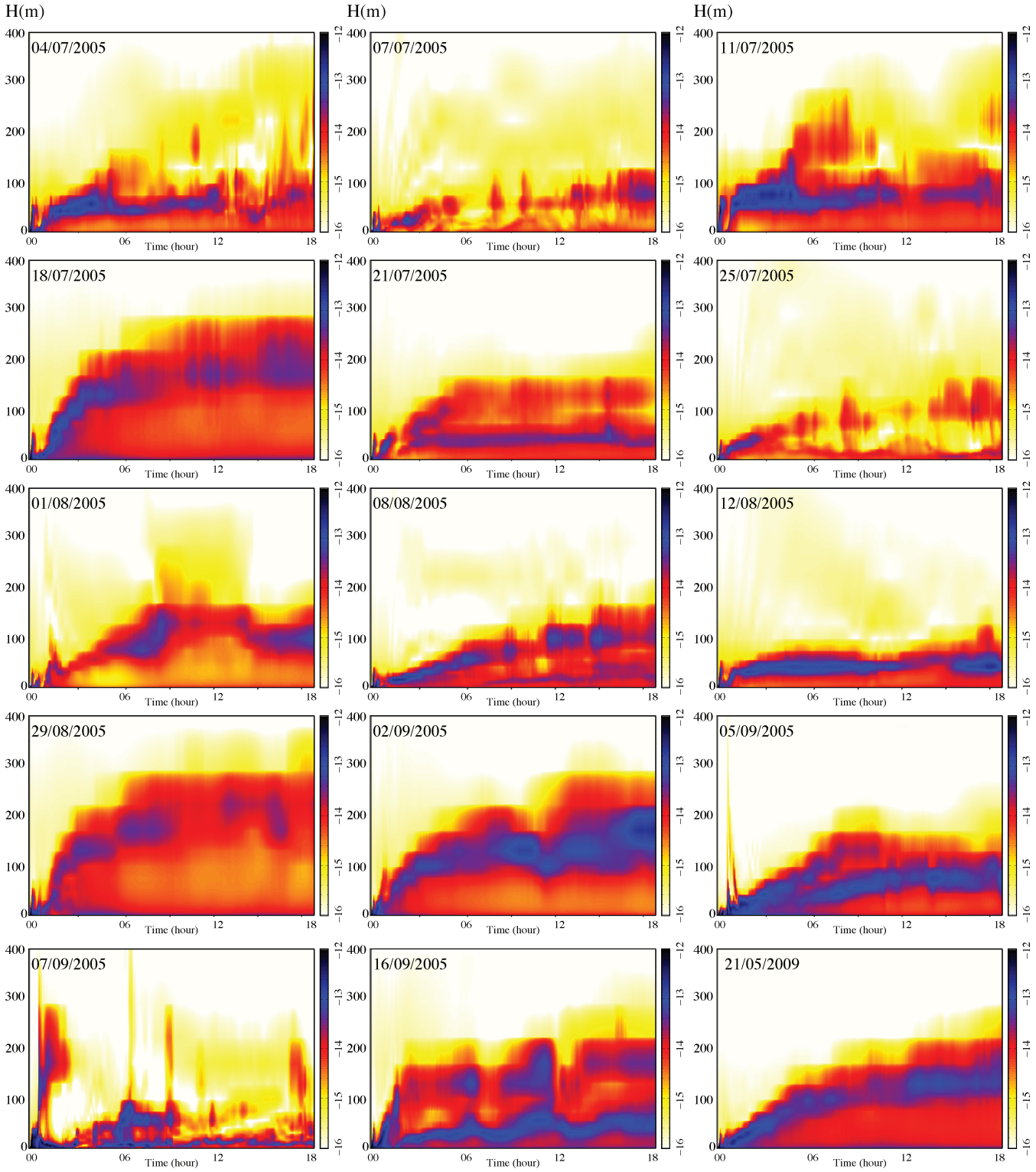

Figure A3. As Fig. A1 but for South Pole.

This paper has been typeset from a TEX/LATEX file prepared by the author.